Kirchhoff prestack depth scalar migration of complete wave field in a simple inhomogeneous weakly anisotropic velocity model: preliminary tests

Václav Bucha
Department of Geophysics, Faculty of Mathematics and Physics, Charles University, Ke Karlovu 3, 121 16 Praha 2, Czech Republic, bucha@seis.karlov.mff.cuni.cz

Summary

We use 3-D ray-based Kirchhoff prestack depth scalar migration to calculate migrated sections in a simple inhomogeneous weakly anisotropic velocity model. The complete seismic wave field is calculated using the Fourier pseudospectral method. Velocity model is composed of two layers separated by a curved interface. The upper layer is inhomogeneous weakly anisotropic and the bottom layer is isotropic. We apply 3-D Kirchhoff prestack depth scalar migration to single-layer velocity model with the same weak anisotropy as in the upper layer of the velocity model used to calculate the recorded wave field. We show and discuss the first results of the migration for complete wave field.

Keywords

Fourier pseudospectral method, 3-D Kirchhoff prestack depth scalar migration, anisotropic velocity model, weak anisotropy, complete wave field

1. Introduction

In this paper we continue in 3-D ray-based Kirchhoff prestack depth scalar migration studies. While in the previous studies we used for migration separate ray-theory elementary waves in this paper we migrate complete wave field calculated by the Fourier pseudospectral method (Tessmer, 1995).

The dimensions of the velocity model, shot-receiver configuration, methods for calculation of the recorded wave field and the migration are the same as in the previous papers by Bucha (e.g., 2012, 2013, 2017), where we studied the sensitivity of the migrated images to incorrect anisotropy, to incorrect gradients of elastic moduli or to incorrect rotation of the tensor of elastic moduli (stiffness tensor).

To compute the synthetic recorded wave field, we use simple anisotropic velocity model composed of two layers separated by one curved interface that is non-inclined in the direction perpendicular to the source-receiver profiles. The inhomogeneous upper layer is weakly anisotropic and the bottom layer is isotropic. The velocity model for the Fourier pseudospectral method is extended by absorption stripes at the sides.

We then migrate complete wave field using 3-D ray-based Kirchhoff prestack depth scalar migration in the single-layer inhomogeneous weakly anisotropic velocity model. The elastic moduli in the velocity model correspond to the upper layer of the velocity model in which the synthetic seismograms have been calculated. For migration we utilize MODEL, CRT, FORMS and DATA software packages (Červený, Klimeš & Pšenčík, 1988; Bulant, 1996; Bucha & Bulant, 2017).

Seismic Waves in Complex 3–D Structures, **28** (2018), 85–96 (ISSN 2336–3827, online at http://sw3d.cz)

2. Anisotropic velocity model

The dimensions of the velocity model and the measurement configuration are derived from the 2-D Marmousi model and dataset (Versteeg & Grau, 1991). The horizontal dimensions of the velocity model are 0 km $\leq x_1 \leq$ 9.2 km, 0 km $\leq x_2 \leq$ 10 km and the depth is 0 km $\leq x_3 \leq$ 3 km. The velocity model is composed of two layers separated by one curved interface (see Figure 1). The curved interface is non-inclined in the direction of the x_2 axis which is perpendicular to the source-receiver profiles.

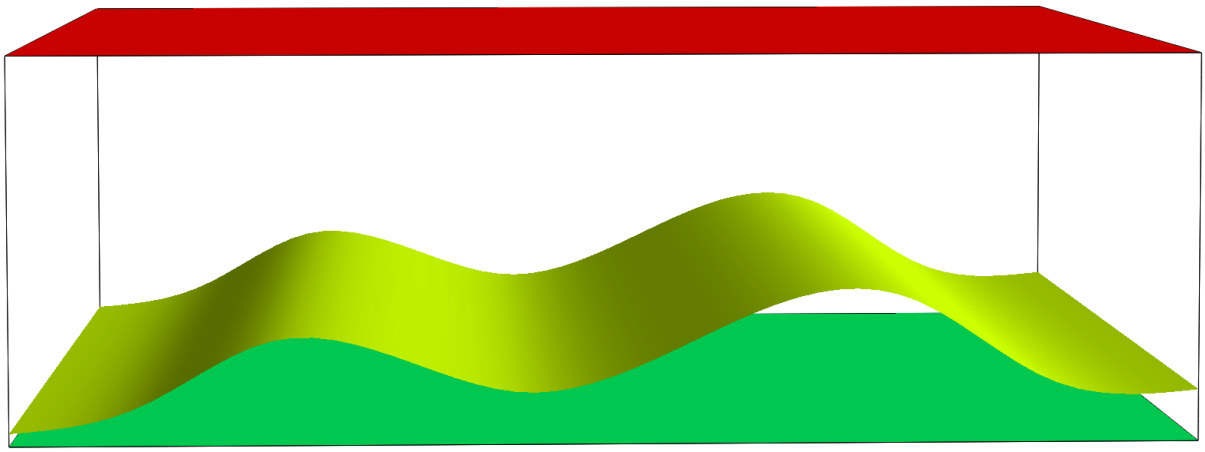

Figure 1. Velocity model with a curved interface and with inhomogeneous weakly anisotropic upper layer. The horizontal dimensions of the velocity model are 0 km $\leq x_1 \leq$ 9.2 km, 0 km $\leq x_2 \leq$ 10 km and the depth is 0 km $\leq x_3 \leq$ 3 km. The velocity model contains one curved interface which is non-inclined in the direction perpendicular to the source-receiver profiles.

The recorded wave field is computed in the velocity model composed of two layers. The medium in the upper layer of the velocity model is inhomogeneous, weakly anisotropic. We use anisotropy proposed by Bulant and Klimeš (2008) in the model QI for the illustration of coupling effects. The model QI coincides with the WA model of Pšenčík and Dellinger (2001). The model QI was also used by Farra and Pšenčík (2010) for a comparison of coupling ray theory based on FORT and standard ray theory results. The QI model is vertically inhomogeneous, transversely isotropic with a horizontal axis of symmetry (HTI). The axis of symmetry is rotated counterclockwise everywhere in the plane (x_1, x_2) by 45^o from the x_1 axis.

The matrix of density-reduced elastic moduli in $\mathrm{km}^2/\mathrm{s}^2$ reads

at $z = 0$ km:

$$\begin{pmatrix} 14.485 & 4.525 & 4.75 & 0.0 & 0.0 & -0.58 \\ & 14.485 & 4.75 & 0.0 & 0.0 & -0.58 \\ & & 15.71 & 0.0 & 0.0 & -0.29 \\ & & & 5.155 & -0.175 & 0.0 \\ & & & & 5.155 & 0.0 \\ & & & & & 5.045 \end{pmatrix}$$

and at $z = 2.9$ km:

$$\begin{pmatrix} 22.08963 & 6.90063 & 7.24375 & 0.0 & 0.0 & -0.88450 \\ & 22.08963 & 7.24375 & 0.0 & 0.0 & -0.88450 \\ & & 23.95775 & 0.0 & 0.0 & -0.44225 \\ & & & 7.86138 & -0.26688 & 0.0 \\ & & & & 7.86138 & 0.0 \\ & & & & & 7.69363 \end{pmatrix}. \quad (1)$$

The P-wave velocity in the isotropic bottom layer is $V_p = 3.6$ km/s and the S-wave velocity is $V_s = V_p/\sqrt{3}$. We migrate in the single-layer velocity model (without the curved interface) with the same weak anisotropy given by matrix (1). The elastic moduli in the velocity model correspond to the upper layer of the velocity model in which the synthetic data have been calculated.

3. Shots and receivers

The measurement configuration is derived from the Marmousi model and dataset (Versteeg & Grau, 1991). The profile lines are parallel with the x_1 coordinate axis. Each profile line has the following configuration: The first shot is 3 km from the left-hand side of the velocity model, the last shot is 8.975 km from the left-hand side of the velocity model, the distance between the shots is 0.025 km, and the depth of the shots is 0 km. The total number of shots along one profile line is 240. The number of receivers per shot is 96, the first receiver is located 2.575 km left of the shot location, the last receiver is 0.2 km left of the shot location, the distance between the receivers is 0.025 km, and the depth of the receivers is 0 km. This configuration simulates a simplified towed streamed acquisition geometry.

The 3-D measurement configuration consists of 81 parallel profile lines, see Figure 2. The interval between the parallel profile lines is 0.025 km.

4. Recorded wave field

To calculate the recorded wave field for 240 shots we apply code FT43DANX by E. Tessmer (Tessmer, 1995). The code is based on the Fourier method (FM), a kind of pseudospectral method (e.g., Kosloff & Baysal, 1982). The code FT43DANX was previously used to test the accuracy of coupling ray theory and standard ray theory results in 3D inhomogeneous, weakly anisotropic media without interfaces (Pšenčík, Farra & Tessmer, 2011; Bulant et al., 2011). This implementation of the FM is applicable to any type and strength of anisotropy. It works equally well in regular as well as in singular regions of the ray method.

The algorithm is based on a regular numerical grid. For simple structures with horizontal layering, the input parameters for velocity model are located in the main ASCII input file. The velocity model for our tests contains a curved interface. In such a case, the input structure for code FT43DANX needs to be gridded and saved in a separate binary file. We performed gridding of the velocity model using MODEL and FORMS packages (Červený, Klimeš & Pšenčík, 1988; Bucha & Bulant, 2017). There are two limitations for setting grid sizes. The first is that the grid size numbers must be factorizable into the factors up to 23, and the FFT algorithm is the more efficient

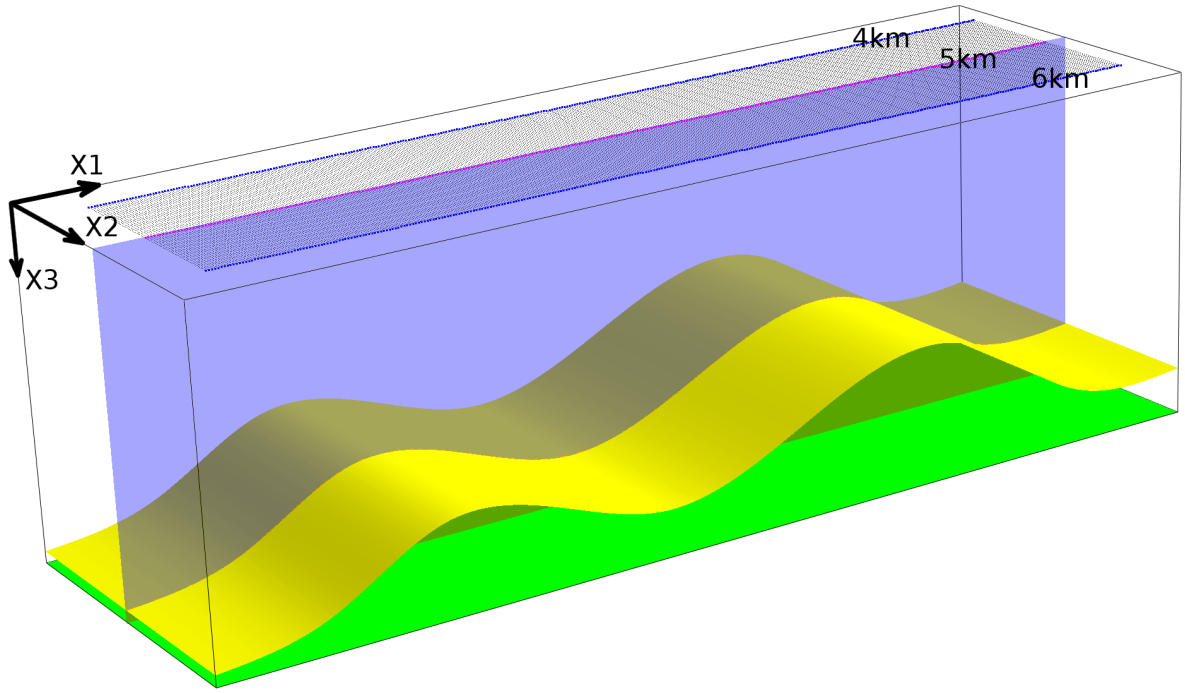

Figure 2. Part of the velocity model with 81 parallel profile lines, the curved interface (yellow) and the bottom velocity model plane (green). The horizontal dimensions of the depicted part of the velocity model are 0 km $\leq x_1 \leq$ 9.2 km, 3.5 km $\leq x_2 \leq$ 6.5 km, the depth is 0 km $\leq x_3 \leq$ 3 km. We compute and stack migrated sections in the 2-D plane (blue) located in the middle of the shot-receiver configuration, at horizontal coordinate $x_2 = 5$ km.

the smaller factors are. The second limitation is connected with the first one, the grid sizes must be odd numbers.

To avoid wrap-around or boundary reflections, the model is surrounded by sponge-like absorbing regions (Cerjan et al., 1985). This requires the numerical grid to be extended at its sides. We present calculation with 20 absorption grid points at the sides of the model. The enlarged model has numerical grid $405 \times 165 \times 189$ grid nodes in the x_1, x_2 and x_3 directions, respectively. The grid steps are 0.025 km. The horizontal dimensions of the velocity model are 0 km $\leq x_1 \leq$ 10.1 km, 0 km $\leq x_2 \leq$ 4.1 km and the depth is 0 km $\leq x_3 \leq$ 4.7 km. The shot is situated 3.45 km from the left-hand side of the enlarged velocity model and the depth of the shot is 1.225 km. The number of receivers per shot is 96. The first receiver is 0.875 km from the left-hand side of the velocity model, the distance between the receivers is 0.025 km, and the depth of the receivers is 1.2 km (see Figure 3).

We use an explosive source for calculation of ray-theory synthetic seismograms. The source-time function is a Gabor wavelet, $\exp[-(2\pi f/\gamma)^2 2t^2]\cos(2\pi f t)$, with the dominant frequency $f = 25$ Hz and $\gamma = 4$. The time step for wave field calculation is 0.003 s and the propagation time starts at 0 s and ends at 2.5 s. The source must be away from the surface. Sources and receivers should be at least 5 grid points away from the absorbing boundaries. Source and receiver positions are specified by grid indices.

Due to the above mentioned limitations and requirements, it is not easy to find the suitable computational grid parameters. Moreover, numerical algorithms based on pseudospectral methods are computationally more expensive than finite-difference methods. We tested the Fourier method with various values of input parameters. The

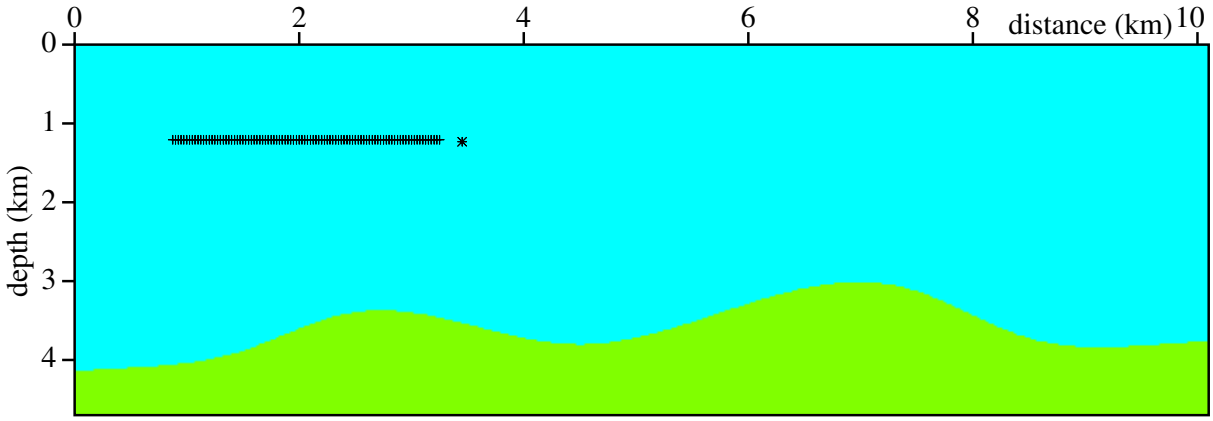

Figure 3. Section of the enlarged velocity model with 20 absorption grid points for the FM calculation. The dimensions of the section are 0 km $\leq x_1 \leq$ 10.1 km and 0 km $\leq x_3 \leq$ 4.7 km. The velocity model contains one curved interface which is non-inclined in the direction perpendicular to the source-receiver profiles. The depth of the shot is 1.225 km. The first receiver is 0.875 km from the left-hand side of the velocity model, and the depth of the receivers is 1.2 km.

results in the paper correspond to our best selection up to date.

The recorded wave field is equal for all parallel profile lines, because the distribution of elastic moduli in the upper layer is vertically inhomogeneous, the bottom layer is homogeneous, and the non-inclined curved interface is independent of the coordinate x_2 perpendicular to the profile lines (2.5-D velocity model, see Figures 1 and 2).

The Fourier method calculates many waves in regions where the ray-theory method fails. For plotting of Fourier method (FM) seismograms, we use the Seismic Unix plotting tools (Cohen & Stockwell, 2013). Seismograms are calculated and plotted up to the time 2.5 s.

To see how complex is complete wave field we display radial (X1), transversal (X2) and vertical (X3) components for common-shot gather 1 (see Figures 4, 5 and 6). Figure 7 shows radial (X1), transversal (X2) and vertical (X3) snapshots for common-shot gather 1.

5. Kirchhoff prestack depth scalar migration

We use the MODEL, CRT, FORMS and DATA software packages for the 3-D Kirchhoff prestack depth scalar migration (Červený, Klimeš & Pšenčík, 1988; Bulant, 1996; Bucha & Bulant, 2017). We migrate the complete wave field.

The migration consists of two-parametric controlled initial-value ray tracing (Bulant, 1999) from the individual surface points, calculating grid values of travel times and amplitudes by interpolation within ray cells (Bulant & Klimeš, 1999), performing the common-shot migration and stacking the migrated images. The shot-receiver configuration consists of 81 parallel profile lines at intervals of 0.025 km (see Figure 2). The first profile line is situated at horizontal coordinate $x_2 = 4$ km and the last profile line is situated at horizontal coordinate $x_2 = 6$ km. For migration we use the single-layer velocity model (without the curved interface) with the same inhomogeneous weak anisotropy as in the upper layer of the velocity model used to calculate the recorded wave field given by matrix (1).

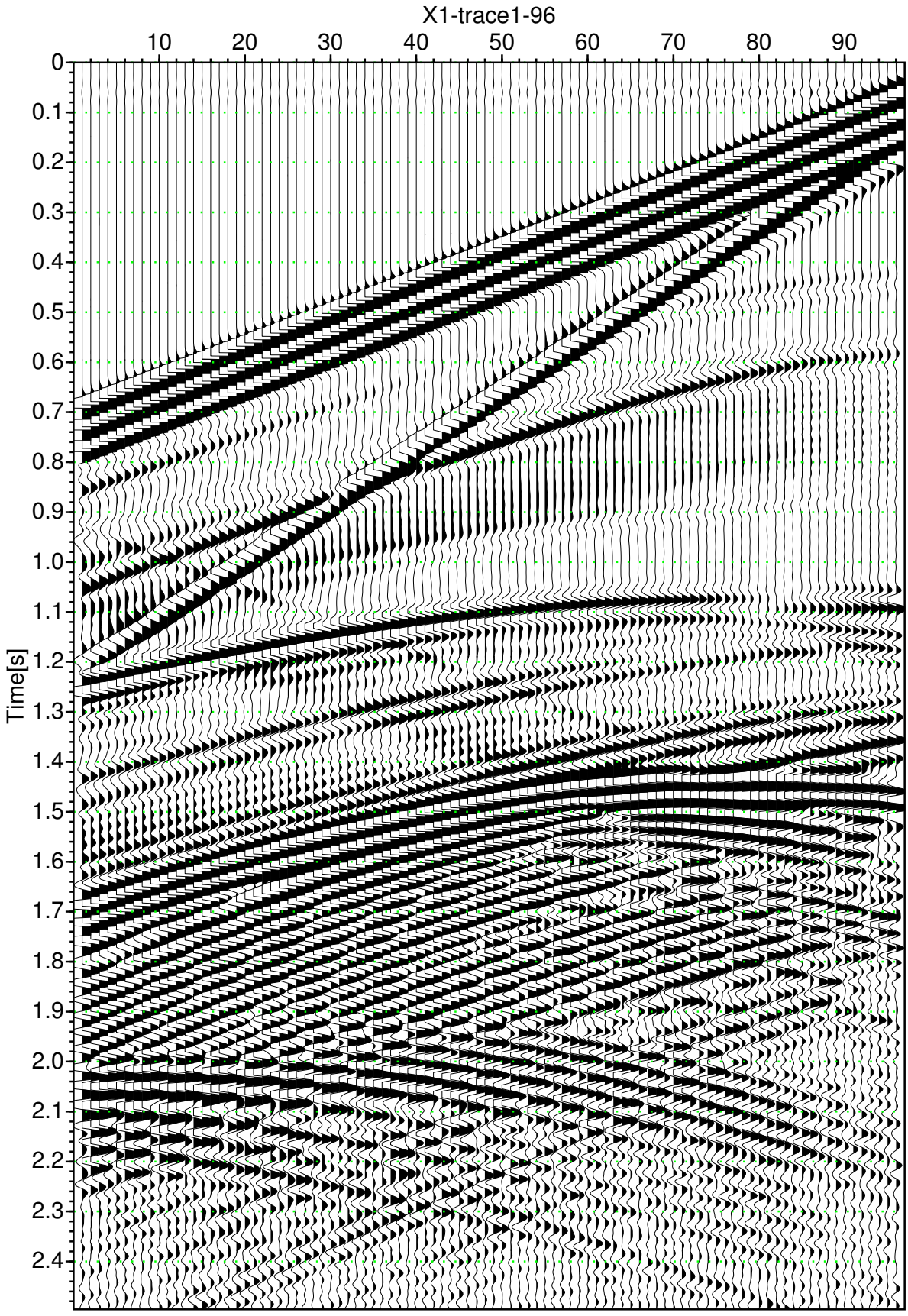

Figure 4. Radial (X1) component of the complete wave field for common-shot gather 1.

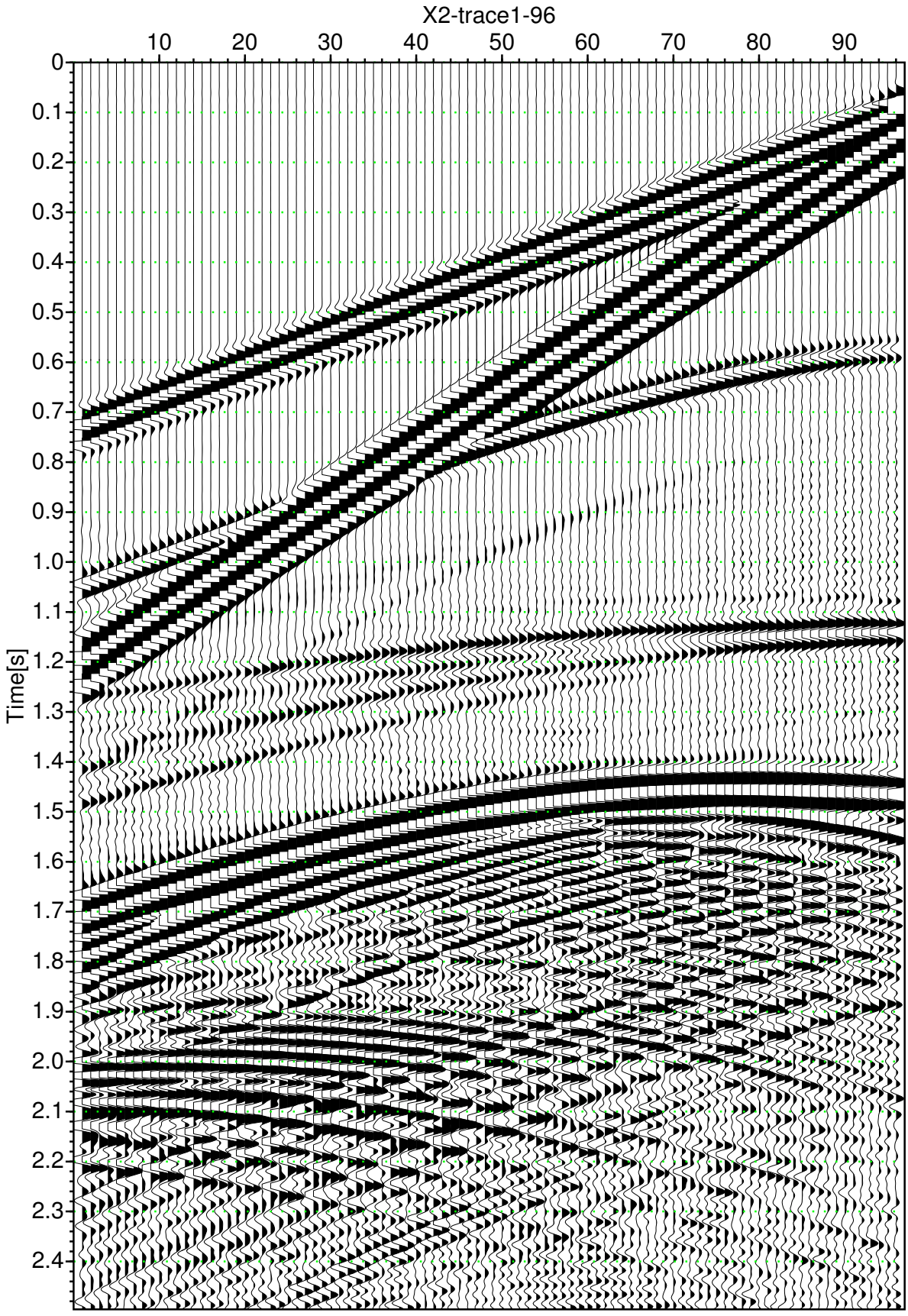

Figure 5. Transversal (X2) component of the complete wave field for common-shot gather 1.

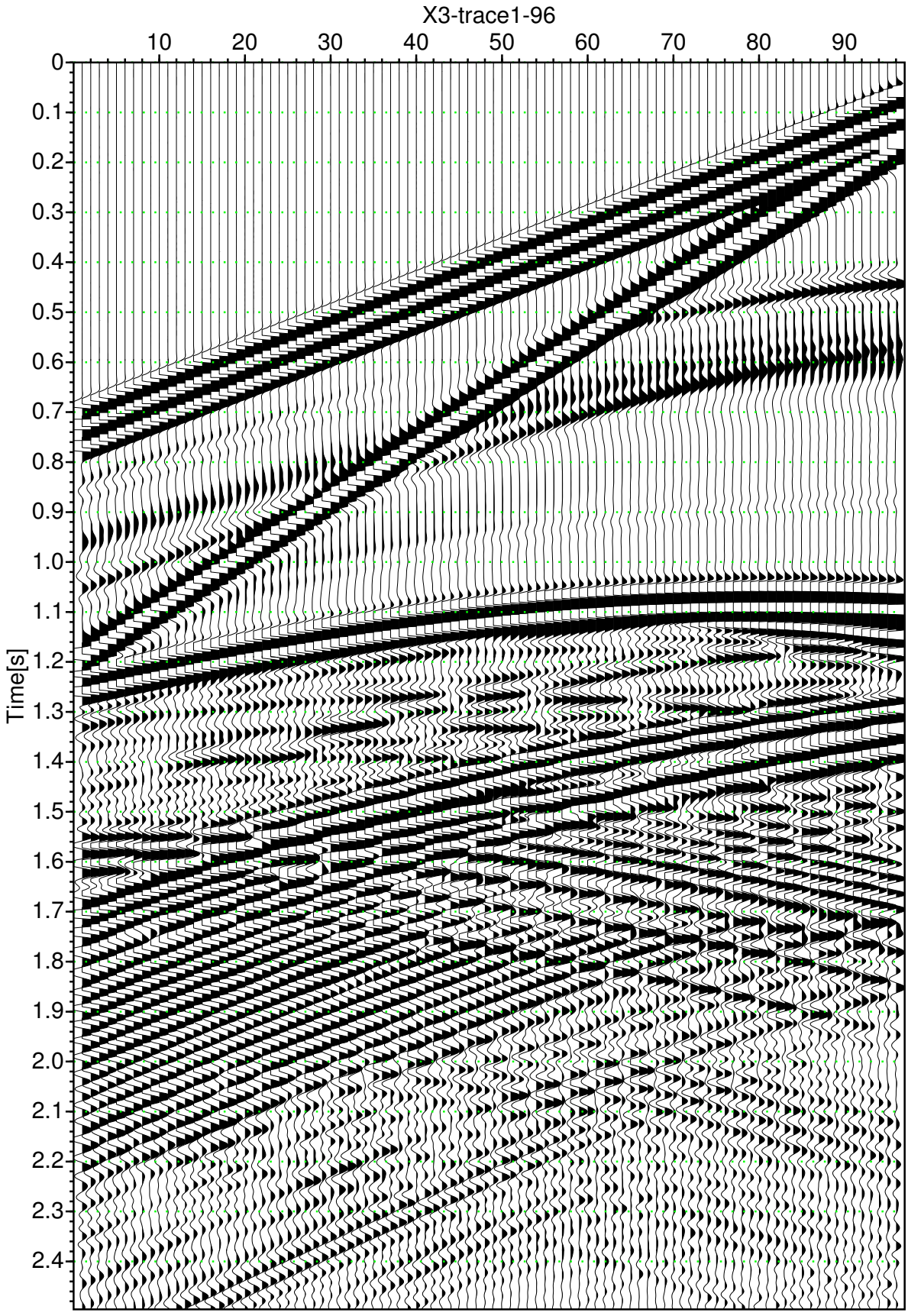

Figure 6. Vertical (X3) component of the complete wave field for common-shot gather 1.

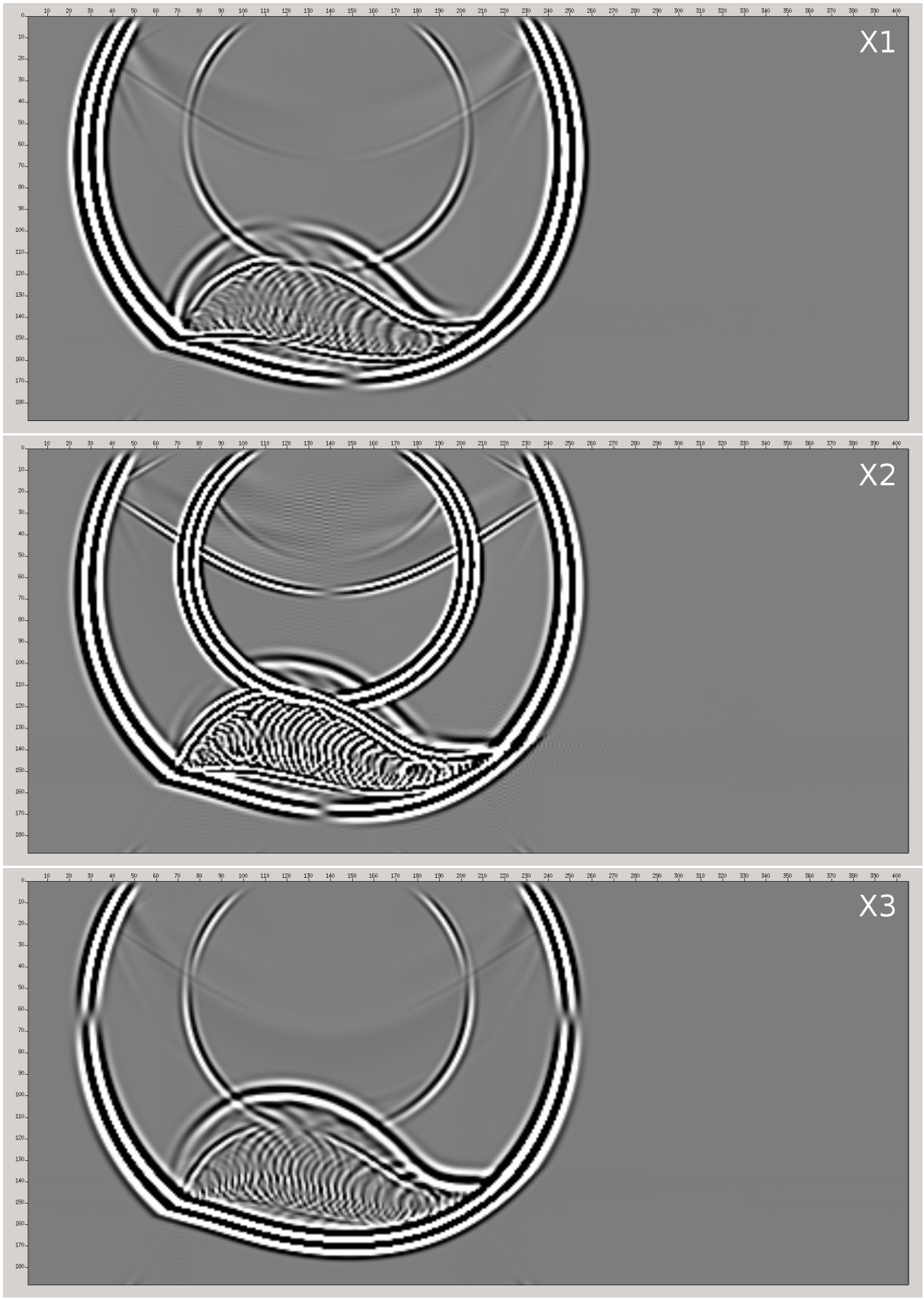

Figure 7. Snapshots of radial (X1), transversal (X2) and vertical (X3) components for common-shot gather 1.

In our tests, we calculate only one vertical image section corresponding to the central profile line ($x_2 = 5$ km, see Figure 2). Although it is only a 2-D profile line, such an image represents one vertical section of full 3-D migrated volume. We form the image by computing and summing the corresponding contributions (images) from all 81 parallel source-receiver lines. While summing the contributions, the constructive interference focuses the migrated interface and the destructive interference reduces undesirable migration artefacts (non-specular reflections). We also use cosine taper to clear artefacts, but some of them remain.

The migration was tested only for one reflected and one converted wave up to date. Figure 8 shows stacked migrated sections calculated for vertical (X3) component of PP reflected wave, radial (X1) component and transversal (X2) component of PS converted wave.

In spite of a complex recorded wave field the migrated interface is in all three sections relatively good. The destructive interference reduces and smudges undesirable migration artefacts. We suppose that dashed and serrated parts of the migrated interface are caused by too big grid step in model parameters for calculation of complete wave field.

6. Conclusions

We have presented preliminary results of Kirchhoff prestack depth scalar migration of complete wave field in a simple inhomogeneous weakly anisotropic velocity model. The results of migration seem to be promising. We shall continue in testing better model gridded parameters.

Acknowledgements

The author thanks Ekkehart Tessmer for providing the Fourier method code. The author also thanks to Ivan Pšenčík and Luděk Klimeš for their help throughout the work on this paper.

The research has been supported by the Grant Agency of the Czech Republic under Contract 16-05237S, by the Ministry of Education of the Czech Republic within Research Project CzechGeo/EPOS LM2015079, and by the members of the consortium "Seismic Waves in Complex 3-D Structures" (see "http://sw3d.cz").

References

Bucha, V. (2012): Kirchhoff prestack depth migration in 3-D simple models: comparison of triclinic anisotropy with simpler anisotropies. *Stud. geophys. geod.*, **56**, 533–552.

Bucha, V. (2013): Kirchhoff prestack depth migration in velocity models with and without vertical gradients: Comparison of triclinic anisotropy with simpler anisotropies. In: *Seismic Waves in Complex 3-D Structures*, **23**, 45–59, online at "http://sw3d.cz".

Bucha, V. (2017): Kirchhoff prestack depth migration in simple models with differently rotated elasticity tensor: orthorhombic and triclinic anisotropy. *J. seism. Explor.*, **26**, 1–24.

Bucha, V. & Bulant, P. (eds.) (2017): SW3D-CD-21 (DVD-ROM). *Seismic Waves in Complex 3-D Structures*, **27**, 133–134, online at "http://sw3d.cz".

Bulant, P. (1996): Two-point ray tracing in 3-D. *Pure appl. Geophys.*, **148**, 421–447. https://doi.org/10.1007/BF00874574

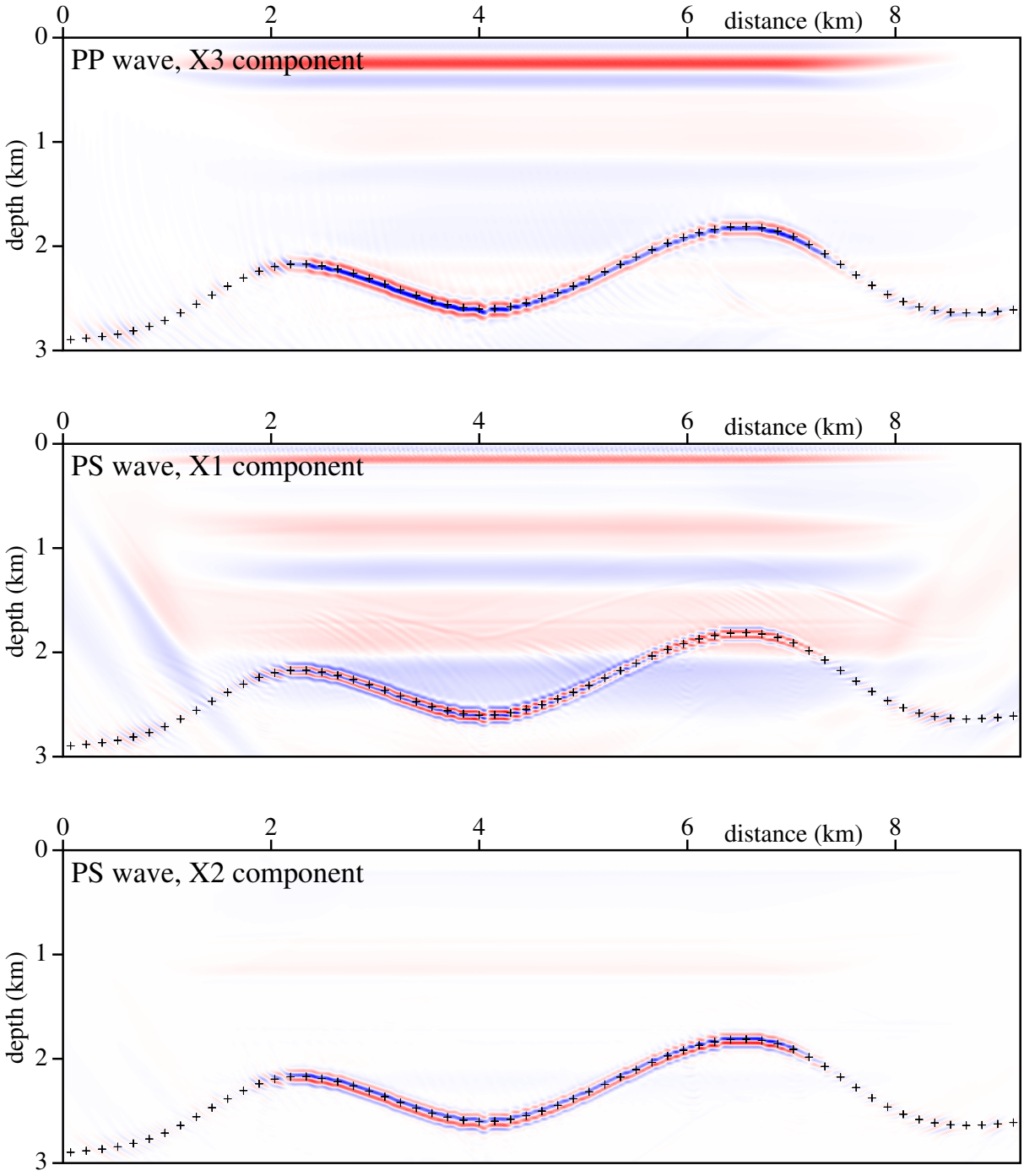

Figure 8. Stacked migrated sections calculated in the weak anisotropy velocity model without interface. Vertical (X3) component of PP reflected wave, radial (X1) component and transversal (X2) component of PS converted wave are used. The elastic moduli in the single-layer velocity model for migration are the same as in the upper layer of the velocity model used to calculate the recorded wave field. 81×240 common-shot prestack depth migrated sections, corresponding to 81 profile lines and 240 sources along each profile line, have been stacked. The crosses denote the interface in the velocity model used to compute the recorded wave field.

Bulant, P. (1999): Two-point ray-tracing and controlled initial-value ray-tracing in 3-D heterogeneous block structures. *J. seism. Explor.*, **8**, 57–75.

Bulant, P. & Klimes, L. (1999): Interpolation of ray-theory travel times within ray cells. *Geophys. J. int.*, **139**, 273–282.

Bulant, P. & Klimeš, L. (2008): Numerical comparison of the isotropic-common-ray and anisotropic-common-ray approximations of the coupling ray theory. *Geophys. J. Int.*, **175**, 357–374.

Bulant, P., Pšenčík, I., Farra, V. & Tessmer, E. (2011): Comparison of the anisotropic-common-ray approximation of the coupling ray theory for S waves with the Fourier pseudo-spectral method in weakly anisotropic models. In: *Seismic Waves in Complex 3-D Structures*, **21**, 167–183, online at "http://sw3d.cz".

Cerjan, C., Kosloff, D., Kosloff, R. & Reshef, M. (1985): A non-reflecting boundary condition for discrete acoustic and elastic wave calculation. *Geophysics*, **50**, 705–708.

Červený, V., Klimeš, L. & Pšenčík, I. (1988): Complete seismic-ray tracing in three-dimensional structures. In: Doornbos, D.J. (ed.), *Seismological Algorithms*, Academic Press, New York, pp. 89–168.

Cohen, J. K. & Stockwell, Jr. J. W. (2013): CWP/SU: Seismic Un*x Release No. 43R5: an open source software package for seismic research and processing, Center for Wave Phenomena, Colorado School of Mines.

Farra, V. & Pšenčík, I. (2010): Coupled S waves in inhomogeneous weakly anisotropic media using first-order ray tracing. *Geophys.J.Int.*, **180**, 405–417.

Kosloff, D. & Baysal, E. (1982): Forward modeling by a Fourier method. *Geophysics*, **47**, 1402–1412.

Pšenčík, I. & Dellinger, J. (2001): Quasi-shear waves in inhomogeneous weakly anisotropic media by the quasi-isotropic approach: a model study. *Geophysics*, **66**, 308–319.

Pšenčík, I., Farra, V. & Tessmer, E. (2011): Comparison of the FORT approximation of the coupling ray theory with the Fourier pseudospectral method. In: *Seismic Waves in Complex 3-D Structures*, **21**, 129–166, online at "http://sw3d.cz".

Tessmer, E. (1995): 3-D seismic modeling of general material anisotopy in the presence of the free surface by a Chebychev spectral method. *Geophys. J. Int.*, **121**, 557–575.

Versteeg, R. J. & Grau, G. (eds.) (1991): The Marmousi experience. *Proc. EAGE workshop on Practical Aspects of Seismic Data Inversion (Copenhagen, 1990)*, Eur. Assoc. Explor. Geophysicists, Zeist.